Advanced Structured Prediction

Editors:

Sebastian Nowozin `Sebastian.Nowozin@microsoft.com`
Microsoft Research
Cambridge, CB1 2FB, United Kingdom

Peter V. Gehler `pgehler@tuebingen.mpg.de`
Max Planck Insitute for Intelligent Systems
72076 Tübingen, Germany

Jeremy Jancsary `jermyj@microsoft.com`
Microsoft Research
Cambridge, CB1 2FB, United Kingdom

Christoph H. Lampert `chl@ist.ac.at`
IST Austria
A-3400 Klosterneuburg, Austria

The MIT Press
Cambridge, Massachusetts
London, England

1 Structured Prediction for Object Boundary Detection in Images

Sinisa Todorovic sinisa@eecs.oregonstate.edu
School of EECS, Oregon State University
Corvallis, OR, USA

This paper presents an overview of our recent work on boundary detection in images using structured prediction. Our input are image edges that are noisy responses of a low-level edge detector. The edges are labeled as belonging to either a boundary or background clutter, thus producing the structured output. The labeling is based on photometric and geometric properties of the edges, as well as evidence of their perceptual grouping. We consider two structured prediction algorithms. First, the policy iteration algorithm, called SLEDGE, sequentially labels the edges, where every labeling step updates features of unlabeled edges based on previously detected boundaries. Second, Heuristic-Cost Search (HC-Search) uncovers high-quality boundary predictions based on a heuristic function, and then selects the prediction with the smallest cost as structured output. On the benchmark Berkeley Segmentation Dataset 500, both algorithms prove robust and effective, and compare favorably with the state of the art in terms of recall and precision. HC-Search outperforms SLEDGE, but at the cost of higher complexity.

1.1 Introduction

This paper presents an overview of our recent work on detecting object boundaries in an arbitrary image. We consider boundary detection that is uninformed about specific objects, and their numbers, scales, and layouts in the scene.

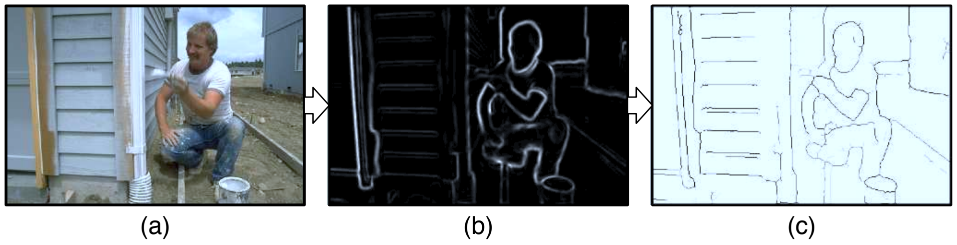

Figure 1.1: Overview: (a) The input image. (b) Edge detectors typically output a probability edge map, which can be thresholded into a set of image edges. (c) Our structured prediction labels every edge as being on or off an object boundary. The darker the boundaries, the higher prediction confidence.

This problem can be cast within the structured prediction framework, where image edges comprising the structured input are mapped to boundary detections comprising the structured output. We use image edges as features suitable for boundary detection. This is because boundaries typically coincide with a subset of edges, and edges provide rich information about the spatial extent and layout of objects in the image. Thus, our structured prediction labels image edges as belonging to either a boundary or background clutter, as illustrated in Figure 1.1.

In this paper, we consider two structured prediction algorithms aimed at optimally combining intrinsic and layout properties of image edges for boundary detection. First, SLEDGE is a policy iteration algorithm, presented in Payet and Todorovic (2013). It sequentially labels the edges, where in each labeling step evidence about the Gestalt grouping of the edges is updated based on previously detected boundaries. Training of SLEDGE is iterative. In each iteration, SLEDGE labels a sequence of edges extracted from each training image. This induces loss with respect to the ground truth. The training sequences are then used as training examples for re-learning SLEDGE in the next iteration, such that the total loss is minimized.

Second, Heuristic-Cost Search (HC-Search) is a structured prediction algorithm based on search in the space of structured outputs (Doppa et al., 2013, 2012). HC-Search uncovers high quality labelings of image edges (i.e., structured outputs), and represents them as nodes of a rooted tree. Links in the tree correspond to moves from one candidate output to another. The goal of HC-Search is to effectively search this tree in order to quickly find an optimal output. To this end, we train a heuristic function to evaluate the moves throughout the search tree, and a cost function to select an optimal node in the tree among the candidates.

Both algorithms prove robust and effective, and compare favorably with the state-of-the-art structured prediction methods, in terms of recall and precision, on the following benchmark datasets: Berkeley segmentation datasets BSD300 and BSD500 (Martin et al., 2001; Arbelaez et al., 2010), Weizmann Horses (Borenstein and Ullman, 2002), and LabelMe (B.Russell et al., 2008). HC-Search gives higher recall and precision, but at the cost of higher complexity than SLEDGE.

In the following, Section 1.2 reviews prior work; Section 1.3 describes the edge detector and edge properties used in this paper; Section 1.4 specifies SLEDGE; Section 1.5 presents HC-Search; and Section 1.6 presents our experimental evaluation.

1.2 Related Work

This section focuses on reviewing prior work on structured prediction, and closely related work on edge-based boundary detection in images.

A standard approach to structured prediction is to learn a cost function $\mathcal{C}(\boldsymbol{x}, \boldsymbol{y})$ for scoring a structured output, $\boldsymbol{y}$, given a structured input, $\boldsymbol{x}$. Computing $\mathcal{C}(\boldsymbol{x}, \boldsymbol{y})$ involves solving the "Argmin" problem, which is to find the minimum cost output for a given input:

$$\text{Argmin:} \quad \hat{\boldsymbol{y}} = \arg\min_{\boldsymbol{y}} \mathcal{C}(\boldsymbol{x}, \boldsymbol{y}). \tag{1.1}$$

Prior work has demonstrated that log-distributions of graphical models – namely, Markov Random Fields (MRF) (Zhu, 1999) or Conditional Random Fields (CRF) (Ren et al., 2008; Maire et al., 2008) – can be used to suitably define $\mathcal{C}(\boldsymbol{x}, \boldsymbol{y})$ in Eq. (1.1) for boundary detection. In general, exactly solving the Argmin problem of Eq. (1.1) is intractable, including the cases when $\mathcal{C}(\boldsymbol{x}, \boldsymbol{y})$ is defined using MRFs or CRFs. This has been addressed using heuristic optimization methods, such as, e.g., loopy belief propagation or variational inference. While such methods have shown some success in practice, the effect of their approximation on learning parameters of the original models of $\mathcal{C}(\boldsymbol{x}, \boldsymbol{y})$ – i.e., MRFs or CRFs – is poorly understood. This is because learning of $\mathcal{C}(\boldsymbol{x}, \boldsymbol{y})$ on training examples typically involves inference as one of the necessary steps.

Another group of methods consider solving the Argmin problem via cascading (Felzenszwalb and McAllester, 2007; Weiss and Taskar, 2010; Munoz et al., 2010), where inference is run in stages from a coarse to fine level of abstraction. These methods, however, have a number of limitations. They place restrictions on the form of $\mathcal{C}(\boldsymbol{x}, \boldsymbol{y})$ to facilitate cascading, which may not be suitable for boundary detection. In particular, they typically ignore the loss function of a problem (e.g., by assuming the Hamming loss), or require that the loss function be decomposable in a way that supports loss augmented inference. In contrast, HC-Search makes minimal assumptions about the loss function, requiring only a “black-box” evaluation of a candidate structured output.

SLEDGE is related to classifier-based methods – including, e.g., SEARN (H. Daumé III et al., 2009), SMiLe (Ross and Bagnell, 2010), and DAgger (Ross et al., 2011). They avoid directly solving the Argmin problem by assuming that structured outputs can be generated by making a series of discrete decisions. Decisions are usually made in a greedy manner using classifiers to produce structured outputs. As a key advantage, these approaches do not make any assumptions about the underlying structure and statistical dependencies of the output variables. However, some decisions in the series are difficult to predict by a greedy classifier, and any intermediate errors may lead to error propagation. SLEDGE mitigates this issue by classifying first those edges which have higher confidence to help make decisions in subsequent ambiguous cases. HC-Search, on the other hand, leverages efficient search spaces over complete outputs, which allows decision making by comparing multiple complete outputs and choosing the best.

HC-Search is also related to Re-Ranking (Collins, 2002), which uses a generative model to propose a k-best list of outputs, which are then ranked by a separate ranking function. Rather than restricting to a generative model for producing candidate outputs, HC-Search leverages generic search over efficient search spaces guided by a learned heuristic function that has minimal representational restrictions, and employs a learned cost function to rank the candidate outputs.

There is a large volume of prior work on edge-based boundary detection. These approaches, first, extract a clutter of image edges, and then use the Gestalt-grouping principles to select and link a subset of the edges into boundaries (Zhu, 1999; Sharon et al., 2001; Zhu et al., 2007; Ren et al., 2008; Kokkinos, 2010b,a). Due to accounting for more global visual information carried by edges as mid-level features, these methods typically outperform patch-based approaches. Another group of related methods track image edges for boundary detection Guy and Medioni (1996); Williams and Thornber (1999); Mahamud et al. (2003); Felzenszwalb and McAllester (2006). They usually resort to heuristic: (i) assumptions about the total number of boundaries; (ii) protocols for tracking (e.g., where to start); and (iii) definitions of edge affinities for tracking. SLEDGE and HC-Search use training examples to estimate these heuristic functions.

1.3 Edge Extraction and Properties

Any low-level edge detector can be used for feature extraction in our approach. In our experiments, we use: (a) Canny edge detector (Canny, 1986), or (b) gPb detector (Maire et al., 2008). gPb produces a probability map of edge saliences. This map is thresholded at all probability levels, and edges extracted using the standard non-maximum suppression. Given a set of image edges, we extract their intrinsic properties and evidence about their Gestalt grouping. In this paper, we use the same edge properties as those described in Payet and Todorovic (2013). Below, we give a brief overview of these properties, for completeness.

1.3.1 Intrinsic Edge Properties

The intrinsic edge properties, $\boldsymbol{\psi}_i$=$[\psi_{i1}, \psi_{i2}]$, include: (a) saliency, ψ_{i1}, and (b) repeatability, ψ_{i2}. Salient edges are likely to belong to boundaries, and repeating edges are more likely to arise from clutter and texture than boundaries.

ψ_{i1} is computed as the mean Pb value along an edge, $\boldsymbol{\psi}_{i1} = \text{mean}_i(Pb)$, for the gPb detector, or the mean of magnitude of intensity gradient along the edge, $\boldsymbol{\psi}_{i1} = \text{mean}_i(\text{gradient})$, for the Canny detector.

For computing ψ_{i2}, we match all pairs of edges in the image. We estimate the dissimilarity of two edges, s_{ij}, as a difference between their Shape Context descriptors (Belongie et al., 2002). After linking all pairs of edges and computing their dissimilarities, Page Rank (Brin and Page, 1998; Kim et al., 2008; Lee and Grauman, 2009) iteratively estimates the degree of repetition of each edge as $\boldsymbol{\psi}_{i2} = (1-\rho) + \rho \sum_j \frac{\boldsymbol{\psi}_{j2}}{\sum_j s_{ik}}$, where $\rho = 0.85$ is the residual probability, and j and k the indices of neighboring edges to edge i. For estimating the neighbors, we construct the Delaunay Triangulation (DT) of all endpoints of the edges. If a pair of endpoints is connected in the DT and directly "visible" to each other without crossing any other edge, then their edges are declared as neighbors. This allows us to estimate proximity and good continuation between even fairly distant edges in the image.

1.3.2 Layout Edge Properties

Layout properties are defined between pairs of neighboring image edges, $\boldsymbol{\phi}_{ij} = [\boldsymbol{\phi}_{ij1}, \ldots, \boldsymbol{\phi}_{ij5}]$, and include standard formulations of the Gestalt principles of grouping (Lowe, 1985; Zhu, 1999; Ren et al., 2008). Let Q_i and Q_j denote the 2D coordinates of the closest endpoints of edges i and j. We estimate:

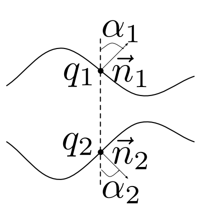

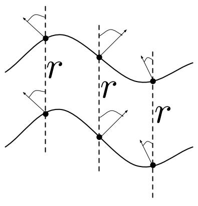

Figure 1.2: (a) The line between symmetric points q_1 and q_2 lying on two distinct edges subtends the same angle $\alpha_1 = \alpha_2$ with the respective edge normals $\vec{n}_1$ and $\vec{n}_2$. (b) Constant distance r between symmetric points of two distinct edges indicates parallelism of the edges.

1. Proximity as $\boldsymbol{\phi}_{ij1} = \frac{2\pi\|Q_i - Q_j\|^2}{\min(\text{len}(i),\text{len}(j))^2}$, where len$(\cdot)$ measures the length of an edge.

2. Collinearity as $\boldsymbol{\phi}_{ij2} = |\frac{d\theta(Q_i)}{dQ_i} - \frac{d\theta(Q_j)}{dQ_j}|$. $\theta(Q) \in [0, 2\pi]$ measures the angle between the x-axis and the tangent of the edge at endpoint Q, where the tangent direction is oriented towards the curve.

3. Co-Circularity as $\boldsymbol{\phi}_{ij3} = |\frac{d^2\theta(Q_i)}{dQ_i^2} - \frac{d^2\theta(Q_j)}{dQ_j^2}|$.

4. Symmetry as $\boldsymbol{\phi}_{ij5} = \text{mean}_{q\in i}\left|\frac{d^2 r(q)}{dq^2}\right|$. As illustrated in Figure 1.2(a), two points $q_1 \in i$ and $q_2 \in j$ are symmetric iff angles $\alpha_1 = \alpha_2$, where α_1 is subtended by line (q_1, q_2) and normal to i, and α_2 is subtended by line (q_1, q_2) and normal to j.

5. Parallelism as $\boldsymbol{\phi}_{ij4} = \text{mean}_{q\in i}\left|\frac{dr(q)}{dq}\right|$. As illustrated in Figure 1.2(b), parallelism is estimated as the mean of distance variations $r(q)$ between points q along edge i and their symmetric points on edge j.

To find symmetric points on two edges, we consider all pairs of points (q_1, q_2), where q_1 belongs to edge 1, and q_2 belongs to edge 2, and compute their cost matrix as a function of α_1 and α_2. We then use the standard Dynamic Time Warping to find the best symmetric points.

By definition, we set $\boldsymbol{\phi}_{ij} = \mathbf{0}$ for all edge pairs (i, j) that are not neighbors.

1.3.3 Helmholtz Principle of Edge Grouping

The Helmholtz principle of grouping (Helmholtz, 1962) is also used as one of the edge properties. It is formalized as the entropy of a layout of edges. When this entropy is low, the edges are less likely to belong to background clutter.

The layout of edges can be characterized using the Voronoi diagram, as presented in Ahuja and Todorovic (2008). Given a set of edges, we first compute the Voronoi tessellation for all pixels along the edges. Then, for each edge i, we find a union of the Voronoi polygons γ_q of the edge's pixels q, resulting in a generalized Voronoi cell, $U_i = \cup_{q \in i} \gamma_q$. The Voronoi cell of edge i defines the relative area of its influence in the image, denoted as $P_i = \text{area}(U_i)/\text{area}(\text{image})$. For n edges, we define the entropy of their layout, H, as

$$H = -\sum_{i=1}^{n} P_i \log P_i. \tag{1.2}$$

Note that P_i depends on the length of i, and its position and orientation relative to the other edges in the image. Since background clutter consists of edges of different sizes, which are placed in different orientations, and at various distances from the other edges, H of the clutter is likely to take larger values than H of object boundaries. From our experiments presented in Payet and Todorovic (2013), H of boundary layouts are in general lower than those of background clutter.

1.3.4 Edge Descriptors

Without losing generality, we assume that from every image we can extract a set of n edges $V = \{i : i = 1, \ldots, n\}$. In our experiments, we set $n = 200$. With every edge $i \in V$, we associate the descriptor $\boldsymbol{x}_i$ defined as

$$\boldsymbol{x}_i = [\boldsymbol{\psi}_i, [\boldsymbol{\phi}_{i1}, \ldots, \boldsymbol{\phi}_{ij}, \ldots], H] \tag{1.3}$$

where $j \in V \backslash \{i\}$. The edge descriptors are used in our structured prediction for boundary detection, as explained in the next two sections.

1.4 Sequential Labeling of Edges

This section describes how to conduct boundary detection as a sequential labeling of image edges.

Let $\boldsymbol{x} = (\boldsymbol{x}_1, \boldsymbol{x}_2, \ldots, \boldsymbol{x}_n) \in \mathcal{X}$ denote a sequence of edge descriptors that are sequentially labeled in n steps, and $\boldsymbol{y} = (y_1, y_2, \ldots, y_n) \in \mathcal{Y}$ denote their corresponding binary labels, $\mathcal{Y} \in \{0, 1\}^n$. SLEDGE sequentially uses a ranking function to select an edge k to be labeled $\hat{y}_k = f(\boldsymbol{x}_k)$, and then updates the descriptors of unlabeled edges, $\boldsymbol{x}_i$, $i = k + 1, \ldots, n$, since they depend on the layout of previously detected boundaries.

SLEDGE uses iterative batch-learning for estimating the structured prediction $f : \mathcal{X} \to \mathcal{Y}$, as summarized in Algorithm 1.1. The structured prediction f is defined as

$$f^{(\tau+1)} = \begin{cases} h^{(\tau+1)} & , \text{ with probability } \beta \in [0,1], \\ f^{(\tau)} & , \text{ with probability } (1-\beta). \end{cases} \tag{1.4}$$

In every learning iteration τ, the result of classification $\hat{\boldsymbol{y}}^{(\tau)} = f^{(\tau)}(\boldsymbol{x})$ is compared with ground truth $\boldsymbol{y}$. This induces loss $l(\hat{\boldsymbol{y}}^{(\tau)}, \boldsymbol{y})$, which is then used to learn a new classifier $h^{(\tau+1)}$, and update $f^{(\tau+1)}$ as in Eq. (1.4) with probability $\beta \in (0,1]$. This definition of $f^{(\tau)}$ amounts to a probabilistic sampling of individual classifiers $h^{(1)}, h^{(2)}, \ldots, h^{(\tau)}$. The classifier sampling is governed by the multinomial distribution. From Eq. (1.4), the probability of selecting classifier $h^{(\tau)}$ in iteration T is

$$\alpha_T^{(\tau)} = \beta^\tau (1-\beta)^{T-\tau}, \quad \tau = 1, 2, \ldots, T. \tag{1.5}$$

After τ reaches the maximum allowed number of iterations, T, the output of learning is the last policy $f^{(T)}$ from which $h^{(1)}$ is eliminated, i.e., the output is $\{h^{(2)}, h^{(3)}, \ldots, h^{(T)}\}$ and their associated sampling probabilities $\{\kappa\alpha_T^{(2)}, \kappa\alpha_T^{(3)}, \ldots, \kappa\alpha_T^{(T)}\}$. The constant κ re-scales the α's, such that $\sum_{\tau=2}^{T} \kappa\alpha_T^{(\tau)} = 1$.

In the following, we specify two loss functions that can be used for learning SLEDGE.

1.4.1 Two Loss Functions of SLEDGE

SLEDGE learns a labeling policy, f, that minimizes the expected loss over all loss-sequences of sequential edge labeling in all training images. In this section, we define two alternative loss functions.

First, we use the standard Hamming loss that counts the total number of differences between predicted and ground-truth labels, $\hat{\boldsymbol{y}} = (\hat{y}_1, \ldots, \hat{y}_n)$ and $\boldsymbol{y} = (y_1, \ldots, y_n)$, as

$$L_H(\hat{\boldsymbol{y}}, \boldsymbol{y}) = \sum_{i=1}^{n} \mathbf{1}\left[\hat{y}_i \neq y_i\right], \tag{1.6}$$

where $\mathbf{1}$ is the indicator function.

Since an error made at any edge carries the same relative weight, the Hamming loss may guide SLEDGE to try to correctly label all small, non-salient edges. To address this problem, we specify another loss function, L_F, that uses the F-measure of recall and precision associated with a specific edge. F-measure is one of the most common performance measures for boundary detection (Martin et al., 2004). It is defined as the harmonic mean of recall and precision of all image pixels that are detected as lying along

Algorithm 1.1 Iterative Batch-Learning of SLEDGE

```
Input:
The set of edges $V_t$ of training images $t = 1, 2, ...$
Ground-truth labels of edges $\boldsymbol{y}_t \in \mathcal{Y}$
Loss-sensitive classifier $h$, and initial $h^{(1)}$
Loss function $l$
Interpolation constant $\beta = 0.1$
Maximum number of learning iterations $T$
Output:
Learned policy $f^{(T)}$

$f^{(1)} = h^{(1)}$
for all training images $t$ do
    for all edges $i \in V_t$ do
        Compute $\boldsymbol{x}_{t,i}^{(1)}$ using intrinsic edge properties
        Set layout edge properties in $\boldsymbol{x}_{t,i}^{(1)}$ to 0
    end for
end for
for $\tau = 1 \dots T$ do
    for all training images $t$ do
        for unlabeled edges in $V_t$ do
            Select unlabeled edge $k \in V_t$ such that $k = \text{argmax}_{i \in V_t} f^{(\tau)}(\boldsymbol{x}_{t,i}^{(\tau)})$
            Compute prediction $\hat{\boldsymbol{y}}_{t,k}^{(\tau)} = f^{(\tau)}(\boldsymbol{x}_{t,k})$
            Update layout properties of unlabeled edges $\boldsymbol{x}_{t,i}^{(\tau)}$
        end for
    end for
    Estimate loss over all training images $l(\hat{\boldsymbol{y}}_t^{(\tau)}, \boldsymbol{y}_t)$
    Learn a new classifier $h^{(\tau+1)} \leftarrow h(\mathcal{X}; l)$
    Compute $f^{(\tau+1)}$ as in Eq. (1.4).
end for
Return $f^{(T)}$ without $h^{(1)}$.
```

an object boundary. A large value of $F(\hat{\boldsymbol{y}}, \boldsymbol{y})$ indicates good precision and recall, and corresponds to a low loss. Thus, we specify

$$L_F(\hat{\boldsymbol{y}}, \boldsymbol{y}) = 1 - F(\hat{\boldsymbol{y}}, \boldsymbol{y}). \tag{1.7}$$

Note that L_H coarsely counts errors at the edge level, while L_F is estimated finely at the pixel level.

1.4.2 Majority Voting of SLEDGE

SLEDGE iteratively learns an optimal policy f, given by Eq. (1.4), which represents a probabilistic mixture of classifiers $\{h^{(\tau)} : \tau = 2, 3, \dots, T\}$. Edges of a new image are sequentially labeled by weighted majority voting of $\{h^{(\tau)}\}$, as described below. Voting decisions of several classifiers has been shown to improve performance and reduces overfitting of each individual classifier (Kittler et al., 1998; Dietterich, 2000; Freund et al., 2001).

For a given edge descriptor $\boldsymbol{x}_i$, we first run all classifiers $\{h^{(\tau)}(\boldsymbol{x}_i)\}$, and then estimate the confidence of edge labeling $\hat{y}_i \in \{0,1\}$ as

$$P(f(\boldsymbol{x}_i) = \hat{y}_i) = \sum_{\tau=2}^{T} \kappa \alpha_T^{(\tau)} P(h^{(\tau)}(\boldsymbol{x}_i) = \hat{y}_i), \tag{1.8}$$

where the constant κ and α's are given by Eq. (1.5), and $P(h^{(\tau)}(\boldsymbol{x}_i){=}y')$ is the confidence of classifier $h^{(\tau)}$ when predicting the label of edge i. Finally, SLEDGE classifies the edge as

$$\hat{y}_i = \operatorname*{argmax}_{y' \in \{0,1\}} P(f(\boldsymbol{x}_i){=}y'). \tag{1.9}$$

1.5 HC-Search

Heuristic-Cost-Search (HC-Search) (Doppa et al., 2012, 2013) performs a search-based structured prediction for a given structured input. Given a set of edges and their descriptors $\boldsymbol{x} = \{\boldsymbol{x}_i : i = 1, \dots, n\}$, HC-Search generates a number of candidate outputs $\tilde{y}$, where input/output pairs $\boldsymbol{s} = (\boldsymbol{x}, \tilde{\boldsymbol{y}})$ represent states of a search space, $\boldsymbol{s} \in \mathcal{S}$, and then selects an optimal state $\hat{\boldsymbol{s}} = (\boldsymbol{x}, \hat{\boldsymbol{y}})$ as the solution. For exploring the search space, HC-Search conducts a search procedure, π, guided by a heuristic function $\mathcal{H}$, whereby new states are generated based on the best previously visited state selected by $\mathcal{H}$. The generation of new states is specified by a generation function, $\boldsymbol{s}' = \mathcal{G}(\boldsymbol{s})$, which is designed to flip low-confidence labels of edges in $\boldsymbol{s}$, and thus generate the new states $\boldsymbol{s}'$. Finally, HC-Search uses a cost function $\mathcal{C}(\boldsymbol{x}, \boldsymbol{y})$ to return the least cost output $\hat{\boldsymbol{y}}$ that is uncovered during the search.

The key elements of HC-Search include:

- Search space over input/output pairs $(\boldsymbol{x}, \hat{\boldsymbol{y}}) \in \mathcal{S}$;
- Search strategy π;
- Heuristic function, $\mathcal{H} : \mathcal{X} \times \mathcal{Y} \mapsto \mathbb{R}$, for guiding the search toward high-quality outputs;
- Cost function, $\mathcal{C} : \mathcal{X} \times \mathcal{Y} \mapsto \mathbb{R}$, for scoring the candidate outputs generated by the search.

Advantages of HC-Search relative to other structured prediction approaches, including CRFs, are as follows. First, it scales gracefully with the complexity of the dependency structure of features. In particular, we are free to increase the complexity of $\mathcal{H}$ and $\mathcal{C}$ (e.g., by including higher-order features) without considering its impact on the inference complexity. The work of Doppa et al. (2012, 2013) shows that the use of higher-order features results in significant improvements. Second, the terms of the error decomposition in Eq. (1.16) can be easily measured for a learned $(\mathcal{H}, \mathcal{C})$ pair, which allows for an assessment of which function is more responsible for the overall error. Third, HC-Search makes minimal assumptions about the loss function, requiring only that we have a "black-box" evaluation of any candidate output. HC-Search can work with non-decomposable loss functions, such as, e.g., F1 loss mentioned in Section 1.4.1.

In the following, we explain all these elements, and then describe how to learn the heuristic and cost functions.

1.5.1 Key Elements of HC-Search

Search Space. A search space $\mathcal{S}$ is defined in terms of two functions: 1) *Initial state function*, $I(\boldsymbol{x})$, returns an initial state in $\mathcal{S}$ for input $\boldsymbol{x}$; and 2) *Generator function*, $\mathcal{G}(\boldsymbol{s})$, returns for any state $\boldsymbol{s}$ a set of new states $\{(\boldsymbol{x}, \tilde{\boldsymbol{y}}_1), \ldots, (\boldsymbol{x}, \tilde{\boldsymbol{y}}_k)\}$ that share the same input $\boldsymbol{x}$.

The specific search space that we investigate leverages boundary predictions made independently for every image edge by the logistic regression classifier. Specifically, our $I(\boldsymbol{x})$ corresponds to the logistic-regression predictions of edge labels. $\mathcal{G}$ generates a set of next states in two steps. First, it identifies a subset of image edges where the classifier has confidence lower than a threshold. When gPb edges are used as input, the threshold is set to 0.5. Second, it generates one successor state for each low-confidence edge i with the corresponding $\tilde{y}_i$ value flipped. We use the conditional probability of the logistic regression as the confidence measure:

$$P(\tilde{y}_i = 1 | \boldsymbol{x}_i; \boldsymbol{w}_{\mathrm{LR}}) = 1/(1 + \exp(-\boldsymbol{w}_{\mathrm{LR}}^\top \boldsymbol{x}_i)), \tag{1.10}$$

where $\boldsymbol{w}_{\mathrm{LR}}$ are parameters of the logistic regression. Note that a particular state may have a large number of successors, depending on $P(\tilde{y}_i = 1 | \boldsymbol{x}_i; \boldsymbol{w}_{\mathrm{LR}})$ values, whereas some other states may have only a few successors.

Search Strategy. The role of the search procedure π is to uncover high-quality outputs, guided by the heuristic function $\mathcal{H}$. Prior work of Doppa et al. (2012, 2013) has shown that greedy search works quite well when used with an effective search space. We investigate HC-Search with greedy search. Given an input $\boldsymbol{x}$, greedy search traverses a path of length τ through the search space, selecting as the next state, the best successor of the current state according to $\mathcal{H}$. Specifically, if $\boldsymbol{s}^{(\tau)}$ is the state at search step τ, π selects $\boldsymbol{s}^{(\tau+1)} = \arg\min_{\boldsymbol{s} \in \mathcal{G}(\boldsymbol{s}^{(\tau)})} \mathcal{H}(\boldsymbol{s})$, where $\boldsymbol{s}^{(0)} = I(\boldsymbol{x})$. We define the maximum allowed number of search steps from one state to another as time bound $\tau_{\max}$.

Note that $\tau_{\max}$ is equal to the number of good candidate states, selected by $\mathcal{H}$ as parents for generating a number of successor states. Thus, the total number of generated states during the search can be much larger than τ.

In this work, we define $\mathcal{H}$ following the standard formulation of CRF in terms of unary and pairwise potential functions, Φ_1 and Φ_2, as

$$\mathcal{H}(\boldsymbol{x},\boldsymbol{y})=\sum_{i\in V}\boldsymbol{w}_{\mathcal{H},1}^{\top}\Phi_1(\boldsymbol{x}_i,y_i)+\sum_{i,j\in V}\boldsymbol{w}_{\mathcal{H},2}^{\top}\Phi_2(\boldsymbol{x}_i,\boldsymbol{x}_j,y_i,y_j), \tag{1.11}$$

where V is the set of input image edges, and $\boldsymbol{w}_{\mathcal{H}}^{\top}=[\boldsymbol{w}_{\mathcal{H},1}^{\top},\boldsymbol{w}_{\mathcal{H},2}^{\top}]$ are parameters of $\mathcal{H}$. As standard, $\Phi_{\text{un}}(\boldsymbol{x}_i,y_i)$ has non-zero elements in the segment that corresponds to label y_i, i.e., $\Phi_{\text{un}}(\boldsymbol{x}_i,0)=[\boldsymbol{x}_i,\boldsymbol{0}]$ or $\Phi_{\text{un}}(\boldsymbol{x}_i,1)=[\boldsymbol{0},\boldsymbol{x}_i]$. The pairwise potential function is defined as

$$\Phi_2(\boldsymbol{x}_i,\boldsymbol{x}_j,y_i,y_j)=\begin{cases}\boldsymbol{0} & ,\ \text{if } y_i=y_j,\\ \exp(-\lambda|\boldsymbol{x}_i-\boldsymbol{x}_j|^2) & ,\ \text{if } y_i\neq y_j,\end{cases} \tag{1.12}$$

where λ is a parameter, set to $\lambda=1$ in our experiments. Φ_2 encourages neighboring edges to take the same label. A similar formulation of the CRF model for boundary detection is specified in Ren et al. (2008); Maire et al. (2008).

Making Predictions. Given $\boldsymbol{x}$, and a prediction time bound τ, HC-Search traverses the search space starting at $I(\boldsymbol{x})$, using the search procedure π, guided by the heuristic function $\mathcal{H}$, until the time bound is exceeded. It then scores each visited state $\boldsymbol{s}$ according to $\mathcal{C}(\boldsymbol{s})$ and returns the $\hat{\boldsymbol{y}}$ of the lowest-cost state as the predicted output.

In this work, we define $\mathcal{C}$ to take the same form as $\mathcal{H}$. In particular, we specify

$$\mathcal{C}(\boldsymbol{x},\boldsymbol{y})=\sum_{i\in V}\boldsymbol{w}_{\mathcal{C},1}^{\top}\Phi_1(\boldsymbol{x}_i,y_i)+\sum_{i,j\in V}\boldsymbol{w}_{\mathcal{C},2}^{\top}\Phi_2(\boldsymbol{x}_i,\boldsymbol{x}_j,y_i,y_j), \tag{1.13}$$

where $\boldsymbol{w}_{\mathcal{C}}^{\top}=[\boldsymbol{w}_{\mathcal{C},1}^{\top},\boldsymbol{w}_{\mathcal{C},2}^{\top}]$ are parameters of $\mathcal{C}$.

1.5.2 Learning Heuristic and Cost Functions

Learning is aimed at training $\mathcal{H}$ and $\mathcal{C}$ such that the error of HC-Search, $\epsilon_{\mathcal{HC}}$, is minimized over training data. $\epsilon_{\mathcal{HC}}$ can be decomposed into two parts: 1) *Generation error*, $\epsilon_{\mathcal{H}}$, due to $\mathcal{H}$ not generating high-quality outputs; and 2) *Selection error*, $\epsilon_{\mathcal{C}|\mathcal{H}}$, conditional on $\mathcal{H}$, due to $\mathcal{C}$ not selecting the best loss output generated by $\mathcal{H}$. Our learning seeks to minimize $\epsilon_{\mathcal{HC}}$ on training data in a greedy stage-wise manner by first training $\mathcal{H}$ to minimize $\epsilon_{\mathcal{H}}$, and then, training $\mathcal{C}$ to minimize $\epsilon_{\mathcal{C}|\mathcal{H}}$ conditioned on $\mathcal{H}$. Below, we specify the error functions minimized in learning.

Let $\boldsymbol{y}^*_{\mathcal{H}}$ denote the best output that HC-Search could possibly return when using $\mathcal{H}$, and $\hat{\boldsymbol{y}}$ denote the output that it actually returns, and $\tilde{\boldsymbol{y}}$ denote candidate outputs, and $\boldsymbol{y}$ denote the ground-truth output. Also, let $\mathcal{Y}_{\mathcal{H}}(\boldsymbol{x})$ be the set of candidate outputs generated using $\mathcal{H}$ for a given input $\boldsymbol{x}$. Then, we define

$$\boldsymbol{y}^*_{\mathcal{H}} = \arg\min_{\tilde{\boldsymbol{y}} \in \mathcal{Y}_{\mathcal{H}}(x)} L(\boldsymbol{x}, \tilde{\boldsymbol{y}}, \boldsymbol{y}), \tag{1.14}$$

$$\hat{\boldsymbol{y}} = \arg\min_{\tilde{\boldsymbol{y}} \in \mathcal{Y}_{\mathcal{H}}(\boldsymbol{x})} \mathcal{C}(\boldsymbol{x}, \tilde{\boldsymbol{y}}), \tag{1.15}$$

where $L(\cdot)$ is a loss function. For HC-Search, we use only the Hamming loss, specified in Eq. (1.6).

We decompose the error of HC-Search as

$$\epsilon_{\mathcal{HC}} = \underbrace{L\left(\boldsymbol{x}, \boldsymbol{y}^*_{\mathcal{H}}, \boldsymbol{y}\right)}_{\epsilon_{\mathcal{H}}} + \underbrace{L\left(\boldsymbol{x}, \hat{\boldsymbol{y}}, \boldsymbol{y}\right) - L\left(\boldsymbol{x}, \boldsymbol{y}^*_{\mathcal{H}}, \boldsymbol{y}\right)}_{\epsilon_{\mathcal{C}|\mathcal{H}}}. \tag{1.16}$$

$\mathcal{H}$ is trained by imitating search decisions made by the true loss available for training data. We run the search procedure π for a time bound of τ for input $\boldsymbol{x}$ using a heuristic equal to the true loss function, i.e. $\mathcal{H}(\boldsymbol{x}, \tilde{\boldsymbol{y}}) = L(\boldsymbol{x}, \tilde{\boldsymbol{y}}, \boldsymbol{y})$. In addition, we record a set of ranking constraints that are sufficient to reproduce the search behavior. For greedy search, at every search step τ, we include one ranking constraint for every state $(\boldsymbol{x}, \tilde{\boldsymbol{y}}) \in \mathcal{C}^{(\tau)} \setminus (\boldsymbol{x}, \tilde{\boldsymbol{y}}_{\text{best}})$, such that $\mathcal{H}(\boldsymbol{x}, \tilde{\boldsymbol{y}}_{\text{best}}) < \mathcal{H}(\boldsymbol{x}, \tilde{\boldsymbol{y}})$, where $(\boldsymbol{x}, \tilde{\boldsymbol{y}}_{best})$ is the best state in the candidate set $\mathcal{C}^{(\tau)}$ (ties are broken by a random tie breaker). The aggregate set of ranking examples is given to a rank learner – namely, SVM-Rank (Joachims, 2006) – to learn $\mathcal{H}$.

$\mathcal{C}$ is trained to score the outputs $\mathcal{Y}_{\mathcal{H}}(\boldsymbol{x})$ generated by $\mathcal{H}$ according to their true losses. Specifically, this training is formulated as a bi-partite ranking problem to rank all the best loss outputs $\mathcal{Y}_{\text{best}}$ higher than all the non-best loss outputs $\mathcal{Y}_{\mathcal{H}}(\boldsymbol{x}) \setminus \mathcal{Y}_{\text{best}}$. For more details, the reader is referred to Doppa et al. (2013).

1.6 Results

This section presents qualitative and quantitative evaluation of SLEDGE and HC-Search on images from the BSD (Martin et al., 2001; Arbelaez et al., 2010), Weizmann Horses (Borenstein and Ullman, 2002), and LabelMe (B.Russell et al., 2008) datasets. BSD300 and BSD500 consist of 300 and 500 natural-scene images, respectively. They are manually segmented by a number of different human annotators. The Weizmann Horses dataset consists of 328 side-view images of horses that are also manually segmented. For the LabelMe dataset, we select the 218 annotated images of the Boston houses 2005 subset. The challenges of these datasets have been extensively discussed in the past, and include, but are not limited to, clutter, illumination variations, occlusion. Below, we present our default training and testing setups.

Training. We train SLEDGE and HC-Search on the 200 training images of BSD300. For each image, we compute the edge probability map gPb (Maire et al., 2008), and threshold the map so as to extract top 200 edges. We compute edge intrinsic and layout properties as described in Section 1.3. For training, we convert the manually annotated boundaries to ground-truth labels for all edges in the training images: if more than 50% of an edge length overlaps with a boundary then the ground-truth label of that edge is 1; otherwise, the label is 0.

For SLEDGE, the initial classifier $h^{(1)}$ is a fully grown C4.5 decision tree, that chooses the split attribute based on the normalized information gain. The attributes considered for $h^{(1)}$ are only the intrinsic parameters ψ_i, specified in Section 1.3.1. In further iterations of SLEDGE, the classifiers $h^{(\tau)}$ are pruned C4.5 decision trees, which are learned on all edge properties. C4.5 pruning uses the standard confidence factor of 0.25. The interpolation constant β, defined in Section 1.4, is set to $\beta = 0.1$. We use F1 loss function, and voting to combine the output of the decision tree classifiers, as described in Section 1.4.2.

For HC-Search, we use SVM-Rank (Joachims, 2006) to learn $\mathcal{H}$ and $\mathcal{C}$ functions. The HC-Search results are obtained for the number of search steps (i.e., time bound) $\tau = 100$.

Testing and Comparison. Performance is measured as the average, pixel-level precision and recall of the boundary map produced by SLEDGE or HC-Search, as defined in Martin et al. (2004). We compare SLEDGE and HC-Search with the latest work that uses standard structured-prediction methods for boundary detection. Namely, for comparison, we use the CRF-based method presented in Maire et al. (2008), and the F^3 boosting method presented in Kokkinos (2010a). For fair comparison, we use the same set of input image edges extracted using the Berkeley segmentation algorithm, as described in Maire et al. (2008).

In the following, we first illustrate a few sample qualitative results of boundary detection by SLEDGE and HC-Search on the BSD dataset. Then, we evaluate SLEDGE and HC-Search using different: initial conditions, edge

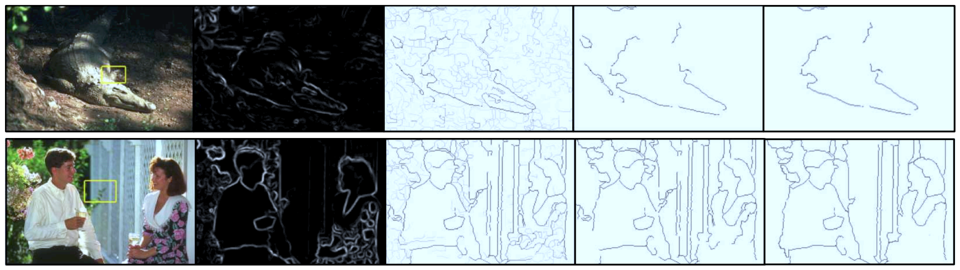

Figure 1.3: **Boundary detection on BSD.** From left to right: Input image; Edge probability map gPb (Maire et al., 2008); Boundary map output by SLEDGE; Boundaries detected by SLEDGE for best F-measure; Boundary map output by HC-Search. The highlighted windows in the original images do not contain salient edges in the input gPb edge map. Yet, both SLEDGE and HC-Search successfully label these non-salient edges as boundaries. SLEDGE and HC-Search perform well on challenging object boundaries amidst texture or low-contrast ramps, e.g.: tip of the alligator's mouth is correctly labeled as boundary, and many salient edges on the woman's dress are correctly labeled as non-boundary.

labeling strategy, classifier type, and loss function.

1.6.1 Qualitative Results

Figure 1.3 shows high accuracy of boundary detection on two sample images from the BSD dataset by SLEDGE and HC-Search. As can be seen, both approaches perform well on challenging object boundaries amidst texture or low-contrast ramps, e.g.: tip of the alligator's mouth is correctly labeled as boundary, and many salient edges on the woman's dress are correctly labeled as non-boundary. Boundary detection is good even in the following cases: (i) when objects have complex textures, e.g., many salient edges on the woman's dress in Figure 1.3(right); (ii) when the boundaries are blurred or jagged, e.g., the tip of the alligator's mouth in Figure 1.3(left); and (iii) when boundaries form complex layouts, e.g., the man's hand in Figure 1.3(right). Filter-based methods, or approaches based on image decimation and smoothing would typically fail to accurately delineate topologically complex layouts of edges where several texture boundaries meet. We are also able to detect boundaries where there is no strong gradient in the input gPb map, e.g., the woman's white collar in Figure 1.3(right).

Figure 1.4 shows the 50 most confident boundaries found by SLEDGE and HC-Search in two example images from the BSD dataset. The boundary detection confidence is color-coded in the HSV space where "warmer" colors mark higher confidence, and "colder" colors indicate lower confidence. As can be seen, both SLEDGE and HC-Search generally are able to find boundaries for non-salient image edges in the gPb map, e.g., see the back

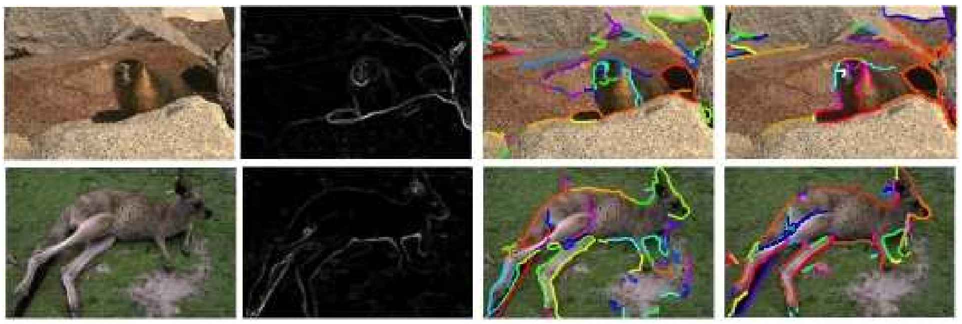

Figure 1.4: **Confidence of boundary detection**. From left to right: Sample image from the BSD dataset; Edge probability map gPb (Maire et al., 2008); 50 most confident boundaries labeled by SLEDGE; 50 most confident boundaries labeled by HC-Search. The confidence of boundary detection is color-coded in the HSV space, where "warm" colors indicate high confidence, and "cold" colors mark low confidence.

of the kangaroo. However, in some cases, SLEDGE wrongly labels salient edges as boundaries when they group well under a certain Gestalt principle. E.g., the edges on the rock texture in Figure 1.4(top) are wrongly labeled as boundaries, since they continue each other well, and thus reinforce their joint labeling as boundaries. HC-Search does not make that mistake on these edges.

Figure 1.5 illustrates the order in which SLEDGE selects edges to label edges in an example image from the BSD dataset. As can be seen, SLEDGE typically first selects to label long, salient edges. Then, SLEDGE seeks to group unlabeled edges with previously identified boundaries. The figure caption explains the underlying Gestalt principle that SLEDGE uses for edge grouping in this example.

SLEDGE and HC-Search compute for every input edge the confidence that it lies on a boundary. Figure 1.6 shows confidence results of SLEDGE and HC-Search on example images from the Weizmann and Labelme datasets. The higher confidence of boundary detection is marked by darker edges. BothSLEDGE and HC-Search accurately assign high confidence to the boundaries of elongated objects, e.g., the electric pole, which are typically challenging for existing approaches. SLEDGE might confuse highly salient edges for boundaries, e.g., the shadow on the horse's neck, and the shadow on the paved area. This is typically because these edges perceptually group well with boundaries, e.g., represent a valid continuation of the horse's front leg. As can be seen, HC-Search gives better results on these two images.

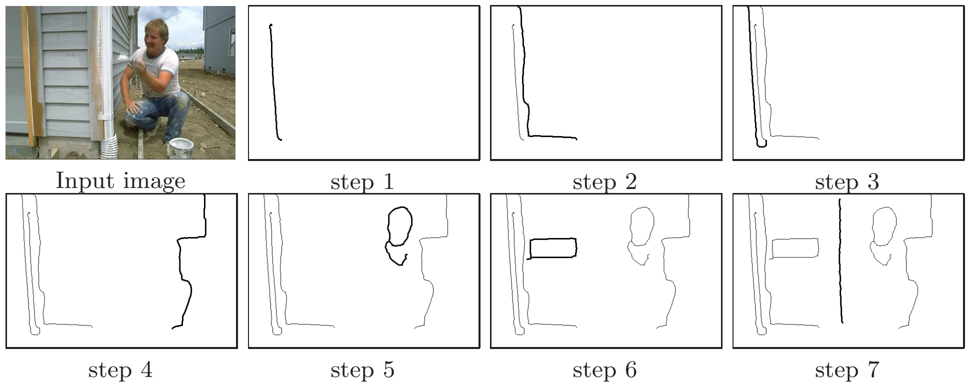

Figure 1.5: Initial sequential labeling steps of SLEDGE for an example image from the BSD dataset. We show only edges from the gPb map (Maire et al., 2008) labeled as boundaries. At step 1, SLEDGE selects a long, prominent edge. At steps 2–4, it selects edges that are parallel to the first boundary, using the grouping principle of parallelism.

1.6.2 Quantitative Evaluation

Following the standard evaluation method of Martin et al. (2004), we convert confidence of boundary detection produced by SLEDGE or HC-Search to a boundary probability map, and use the map for performance evaluation.

First, we evaluate the boundary map output by SLEDGE and HC-Search using different types of input edges. We use the same type of input edges for training and testing of our algorithms. Figure 1.7 shows our precision and recall for image edges obtained with the Canny detector (Canny, 1986), and the gPb detector (Maire et al., 2008). Sequential labeling significantly improves performance for all edge detectors, especially in the high-recall-low-precision regime. This demonstrates that SLEDGE does not require a very good initial set of edges for good performance. We note however that the higher the precision of original input edges, the higher the precision of output boundaries. For example, Figure 1.7 shows that the precision of gPb+SLEDGE is higher than the precision of Canny+SLEDGE. HC-Search also improves boundary detection over the performance of edge detectors, and outperforms SLEDGE.

Figure 1.8 shows the average precision and recall of gPb+SLEDGE, gPb+HC-Search, gPb of (Maire et al., 2008), and the F^3 boosting method of (Kokkinos, 2010a) on the following datasets: BSD 300, BSD 500, Weizmann Horses and LabelMe. SLEDGE and HC-Search are trained on the standard 200 training images from the BSD, as the competing approaches. As can be seen, both SLEDGE and HC-Search outperform the standard structured prediction methods – namely, the CRF-based gPb (Maire et al., 2008), and

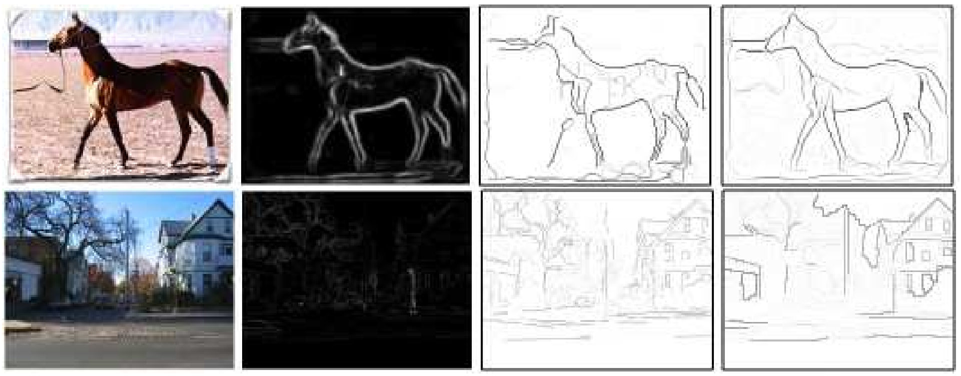

Figure 1.6: **Boundary detection on the Weizmann dataset (top) and the LabelMe dataset (bottom).** From left to right: Input image; Edge probability map gPb (Maire et al., 2008); Boundary detection confidence map output by SLEDGE; Boundary detection confidence map output by HC-Search.

F^3 boosting (Kokkinos, 2010a) – on all the datasets. HC-Search outperforms SLEDGE.

1.6.3 Evaluating Particular Aspects of SLEDGE

This section presents the effect of different design choices on the performance of SLEDGE.

Initial conditions. The early errors of SLEDGE in the sequence might be critical, because they could sequentially propagate to the entire sequence. To test this aspect of our algorithm, we compare our default setup with the following variant of SLEDGE. We create 100 different initial configurations by randomly picking b true boundaries as the initial set of correctly labeled edges. The randomization serves to eliminate any bias in picking certain boundaries (e.g., long ones). Then, we let SLEDGE continue labeling the remaining edges. The pairwise and global features are computed based on the initial set of randomly selected true boundaries. Finally, we compute recall and precision averaged over these 100 distinct initializations. These tests serve to evaluate SLEDGE performance when there is no error at the beginning of the labeling sequence. Table 1.1 shows the average increase in recall and precision, at equal error rate, relative to those of our default setup, for $b = 2, 4, 6$. As can be seen, when errors at the beginning of the labeling sequence are manually eliminated, our performance gain is relatively small. This suggests that our default setup is relatively insensitive to initial labeling errors.

Edge labeling strategy. We test how performance varies when we allow

	$b = 2$	$b = 4$	$b = 6$
Increase in recall [%]	21 ± 2.3	33 ± 2.4	61 ± 1.84
Increase in precision [%]	23 ± 3.5	25 ± 1.9	49 ± 2.1

Table 1.1: **Initial conditions.** Increase in recall and precision in %, at equal error rate, relative to those of our default setup, averaged over 100 random initializations consisting of $b \in \{2, 4, 6\}$ true boundaries as the initial set of correctly labeled edges.

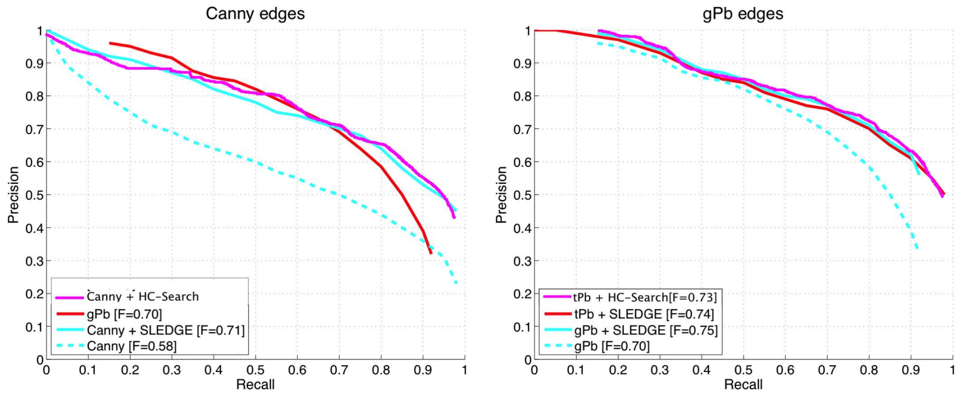

Figure 1.7: **Improvement in boundary detection.** We evaluate boundary detection on the BSD300 dataset in two cases: outputs of edge detectors are input to SLEDGE and HC-Search (solid lines), and outputs of edge detectors are simply declared as boundary detection without using our algorithms (dashed line). The detectors include: (top) Canny (Canny, 1986), and (bottom) gPb (Maire et al., 2008). Training and testing are performed with the same type of edges, e.g., for testing SLEDGE on Canny edges, we trained SLEDGE on Canny edges. Both SLEDGE and HC-Search improve the precision of the input set of edges. HC-Search outperforms SLEDGE.

SLEDGE to continue relabeling edges after all the edges have already been labeled once. Specifically, after all edges have been visited, we remove them from the labeled set and send them to the unlabeled set. The pairwise and global features are still computed based on the current labeling of boundaries. We iterate SLEDGE until it reaches convergence, i.e., no edge changes the label. On the 100 test images of the BSD300, at equal error rate, SLEDGE with relabeling improves by 0.2% in precision, and by 0.5% in recall, relative to the performance of the default SLEDGE with just one labeling pass. Thus, allowing edges to be relabeled, in our approach, only marginally improves precision and recall, but increases complexity. Therefore, it seems that the iterative relabeling of edges is not justified in our approach.

Classifiers. From our experiments, a non-linear classifier is more suitable

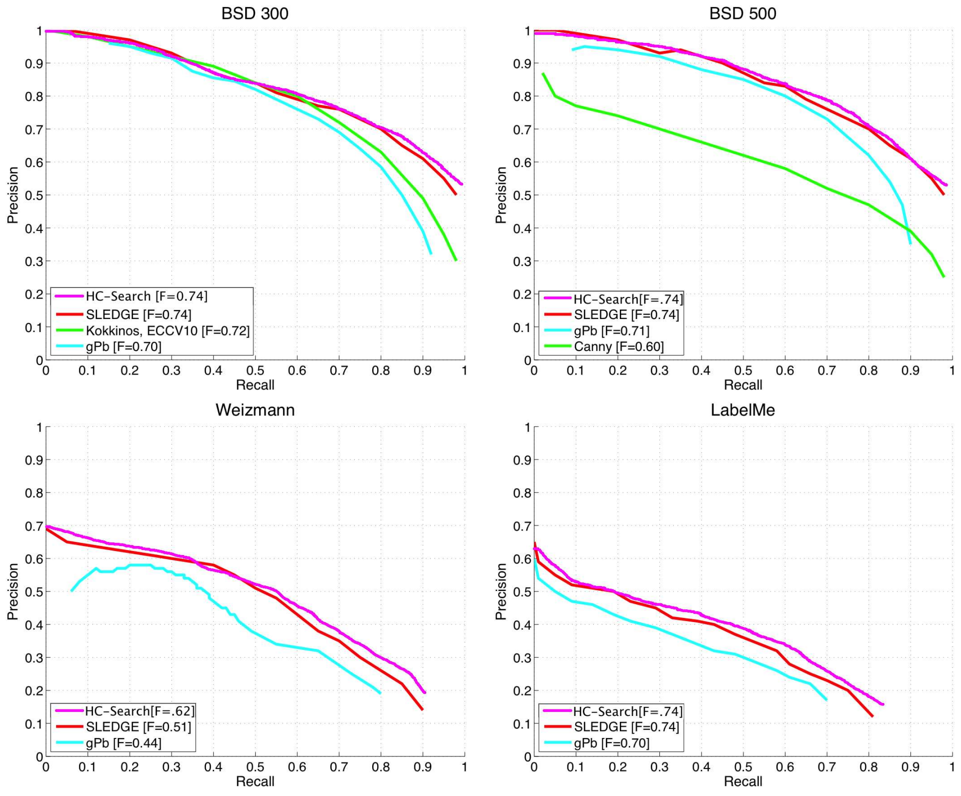

Figure 1.8: **Boundary detection.** Precision and recall of gPb+SLEDGE, gPb+HC-Search, and gPb (Maire et al., 2008) on the datasets: BSD 300 (Martin et al., 2001), BSD 500 (Arbelaez et al., 2010), Weizmann Horses (Borenstein and Ullman, 2002) and LabelMe (B.Russell et al., 2008). For BSD 300, we also show a comparison with the method of Kokkinos (2010a). We outperform gPb on all four datasets, and obtain a better F-measure than Kokkinos (2010a) on the BSD 300.

than a linear one for separating boundaries from background edges. Classification accuracy of SLEDGE with decision trees compared to that of SLEDGE with a linear SVM-type classifier is 91% vs. 72%. For training SVMs (as in the case of decision trees), we use a balanced number of positive and negative examples – the under-sampling procedure mentioned in Section 1.4.2-Remark – with the complexity parameter $C = 1.0$. When more sophisticated classifiers are used, e.g. SVM with RBF and random forests, we observe only a relatively small gain in accuracy over the decision tree, which does not justify the increase in complexity. Indeed, the total computation time primarily depends on the complexity of the chosen classifier as all classifiers have to be run at each iteration of SLEDGE.

Loss functions. Figure 1.9(a) shows the performance of SLEDGE when

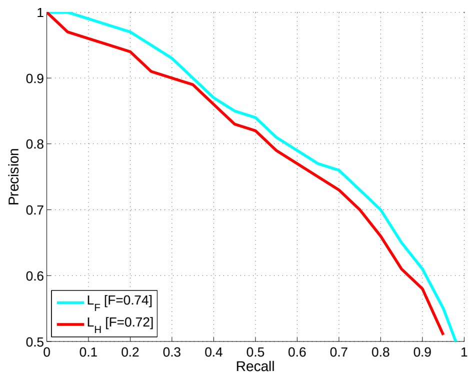

(a) Loss functions

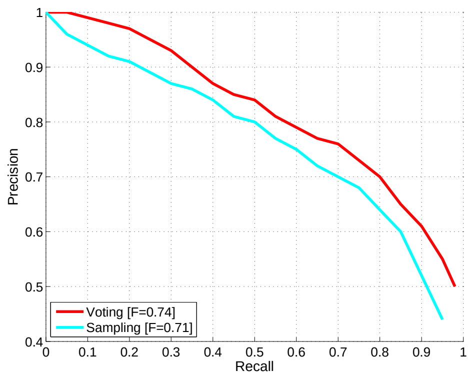

(b) Interpolation schemes

Figure 1.9: Performance of SLEDGE on the BSD 300 when: (a) Using the loss function L_H or L_F, given by Eq. (1.6) and Eq. (1.7); L_H coarsely counts errors at the edge level, while L_F is a loss estimated finely at the pixel level. (b) Making decisions using classifier sampling or voting.

using the loss function L_H or L_F, specified in Section 1.4.1. L_H coarsely counts errors at the edge level, while L_F is a loss estimated finely at the pixel level. SLEDGE with L_F produces boundaries with slightly better precision than SLEDGE with L_H. SLEDGE with L_F also runs about 3 times faster than SLEDGE with L_H.

Interpolation scheme. We stop learning new classifiers when the average performance on the training data does not change. For the BSD 300, this happens after about 10 iterations. Figure 1.9(b) compares the performance of SLEDGE with these 10 classifiers for two types of making decisions by: (i) Sampling the classifiers; and (ii) Weighted voting of the classifiers, as described in Section 1.4.2. As can be seen, voting outperforms sampling.

1.6.4 Evaluating Particular Aspects of HC-Search

This section presents the effect of different design choices on the performance of HC-Search. We evaluate our sensitivity to the time bound, $\tau_{\max}$, i.e., the number of search steps that are allowed before making the final prediction. Recall that $\tau_{\max}$ is equal to the number of states selected by the heuristic function $\mathcal{H}$ as parents for generating successor states, as described in Section 1.5.1. The total number of generated states during HC-Search can be much larger than $\tau_{\max}$.

Figure 1.10 shows the plots of precision and recall of HC-Search for increasing time bound $\tau_{\max}$. The plots show four types of curves: LL-Search, HL-Search, LC-Search and HC-Search. LL-Search uses the loss function as both the heuristic and the cost function, and thus serves as an upper

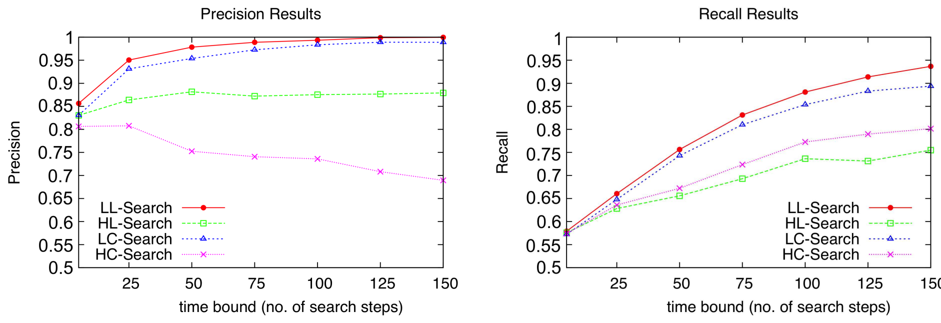

Figure 1.10: The plots of precision and recall of HC-Search on the BSD 300 versus the allowed number of search steps.

bound on the performance. HL-Search uses the learned heuristic function, and the loss function as cost function, and thus serves to illustrate how well the learned heuristic $\mathcal{H}$ performs in terms of the quality of generated outputs. LC-Search uses the loss function as an oracle heuristic, and learns a cost function to score the outputs generated by the oracle heuristic. From Figure 1.10, for HC-Search, we see that as $\tau_{\max}$ increases, precision drops, but recall improves up to a certain point before decreasing. This is because as $\tau_{\max}$ increases, the generation error ($\epsilon_{\mathcal{H}}$) will monotonically decrease, since strictly more outputs will be encountered. Simultaneously, difficulty of cost function learning can increase as $\tau_{\max}$ grows, since it must learn to distinguish among a larger set of candidate outputs. In addition, we can see that the LC-Search curve is very close to the LL-Search curve, while the HL-Search curve is far below the LL-Search curve. This suggests that the overall error of HC-Search, $\epsilon_{\mathcal{HC}}$, is dominated by the heuristic error $\epsilon_{\mathcal{H}}$. A better heuristic is thus likely to lead to better performance overall. One could try to improve the heuristic error in several ways, including flipping multiple patch labels, training heuristic function with more advanced imitation learning algorithms (e.g., DAgger) and learning non-linear ranking functions (e.g., Boosted Regression Trees). We plan to investigate these directions in future.

1.6.5 Running-time

Training SLEDGE on 200 BSD training images takes about 24 hours, on a 2.66GHz, 3.4GB RAM PC. Computing the boundary probability map by SLEDGE for a new image takes 20-40sec, depending on the image content.

Training heuristic $\mathcal{H}$ and cost $\mathcal{C}$ functions on 200 BSD training images takes about 3-4 hours, on the same PC. For the maximum allowed number of search steps $\tau_{\max} = 100$, boundary detection by HC-Search in a new image takes about 2 minutes.

Our code is implemented in MATLAB, and is not fully optimized for efficiency.

1.7 Conclusion

We have presented two structured prediction approaches to boundary detection in arbitrary images, called SLEDGE and HC-Search. Both approaches take as input salient edges, and label these edges as belonging to a boundary. SLEDGE is a sequential labeling algorithm, which learns how to optimally combine Gestalt grouping cues and intrinsic edge properties for boundary detection. HC-Search is a search based algorithm, which greedily explores the space of candidate solutions guided by the heuristic function, and then selects the minimum cost solution from all the candidates.

Our empirical evaluation demonstrates that both SLEDGE and HC-Search outperform standard structured prediction approaches to boundary detection on the benchmark datasets – specifically, the CRF-based method gPb (Maire et al., 2008), and F^3 boosting (Kokkinos, 2010a). This is, in part, because both SLEDGE and HC-Search avoid directly solving the Argmin problem of structured prediction by generating structured outputs through: (i) Making a series of discrete decisions in the case of SLEDGE; or (ii) Searching the output space in the case of HC-Search. Both SLEDGE and HC-Search employ training data to explicitly *learn how to conduct inference* through making sequential decisions or searching the output space. This learning for inference seems to improve upon common practice to use heuristic approximations for solving the NP-hard Argmin problem. As a key advantage over the other structured prediction methods, SLEDGE and HC-Search do not make strong assumptions about the underlying structure and statistical dependencies of the output variables.

We have observed that SLEDGE tends to favor good continuation of strong edges, which works well in most cases, but fails when there is an accidental alignment of object and background edges (e.g., shadows).

Our experimental results indicate that the overall error of the HC-Search approach is dominated by the heuristic error. One could try to further improve our current results with HC-Search by improving the heuristic function. We are currently investigating this direction by employing more effective search spaces, advanced imitation learning algorithms, and non-linear representations (e.g., Boosted Regression Trees) for the heuristic and cost functions. A better search space can be constructed by flipping the labels of multiple edges rather than one at a time, thereby reducing the search depth for imitation learning. In this paper, we have used exact imitation to generate training examples for learning the heuristic function. Perhaps using DAgger (Ross et al., 2011) would be a better method. Finally, we have used SVM Rank to learn the heuristic and cost functions, but one could try to use other rank learners such as boosting and trees.

Acknowledgements

This research has been sponsored in part by grant NSF IIS 1302700.

1.8 References

N. Ahuja and S. Todorovic. Connected segmentation tree – a joint representation of region layout and hierarchy. In *Conf. Computer Vision Pattern Recognition*, 2008.

P. Arbelaez, M. Maire, C. Fowlkes, and J. Malik. Contour detection and hierarchical image segmentation. *IEEE Trans. PAMI*, 99(RapidPosts), 2010.

S. Belongie, J. Malik, and J. Puzicha. Shape matching and object recognition using shape contexts. *IEEE Trans. PAMI*, 24(4):509–522, 2002.

E. Borenstein and S. Ullman. Class-specific, top-down segmentation. In *European Conf. Computer Vision*, volume 2, pages 109–124, 2002.

S. Brin and L. Page. The anatomy of a large-scale hypertextual web search engine. In *Seventh International World-Wide Web Conference (WWW 1998)*, 1998.

B.Russell, A. Torralba, K. Murphy, and W. Freeman. LabelMe: a database and web-based tool for image annotation. *Int. J. Computer Vision*, 77(1-3):157–173, 2008.

J. Canny. A computational approach to edge detection. *IEEE Trans. PAMI*, 8(6): 679–698, 1986.

M. Collins. Ranking algorithms for named entity extraction: Boosting and the voted perceptron. In *Proceedings of Association for Computational Linguistics*, 2002.

T. Dietterich. Ensemble methods in machine learning. In *Lecture Notes in Computer Science*, pages 1–15, 2000.

J. Doppa, A. Fern, and P. Tadepalli. Output space search for structured prediction. In *Int. Conf. Machine Learning*, 2012.

J. Doppa, A. Fern, and P. Tadepalli. HC-Search: Learning heuristics and cost functions for structured prediction. In *AAAI Conference on Artificial Intelligence*, 2013.

P. Felzenszwalb and D. McAllester. A min-cover approach for finding salient curves. In *Conf. Perceptual Organization Computer Vision*, 2006.

P. Felzenszwalb and D. McAllester. The generalized A* architecture. *Journal of Artificial Intelligence Research*, 29:153–190, 2007.

Y. Freund, Y. Mansour, and R. Schapire. Why averaging classifiers can protect against overfitting. In *Int. Workshop on Artificial Intelligence and Statistics*, 2001.

G. Guy and G. Medioni. Inferring global perceptual contours from local features. *Int. J. Computer Vision*, 20(1-2):113–133, 1996.

H. Daumé III, J. Langford, and D. Marcu. Search-based structured prediction. *Machine Learning Journal*, 75(3):297–325, 2009.

H. Helmholtz. *Treatise on physiological optics.* New York: Dover; (first published in 1867), 1962.

T. Joachims. Training linear SVMs in linear time. In *Int. Conf. Knowledge Discovery and Data Mining*, pages 217–226, 2006.

G. Kim, C. Faloutsos, and M. Hebert. Unsupervised modeling of object categories using link analysis techniques. In *Conf. Computer Vision Pattern Recognition*, June 2008.

J. Kittler, M. Hatef, R. Duin, and J. Matas. On combining classifiers. *IEEE Trans. PAMI*, 20:226–239, 1998.

I. Kokkinos. Boundary detection using F-measure-, Filter- and Feature- (F^3) boost. In *European Conf. Computer Vision*, 2010a.

I. Kokkinos. Highly accurate boundary detection and grouping. In *Conf. Computer Vision Pattern Recognition*, 2010b.

Y. Lee and K. Grauman. Shape discovery from unlabeled image collections. In *Conf. Computer Vision Pattern Recognition*, 2009.

D. Lowe. *Perceptual Organization and Visual Recognition.* Kluwer Academic Publishers, Norwell, MA, USA, 1985.

S. Mahamud, L. Williams, K. Thornber, and K. Xu. Segmentation of multiple salient closed contours from real images. *IEEE Trans. PAMI*, 25(4):433–444, 2003.

M. Maire, P. Arbelaez, C. Fowlkes, and J. Malik. Using contours to detect and localize junctions in natural images. In *Conf. Computer Vision Pattern Recognition*, 2008.

D. Martin, C. Fowlkes, D. Tal, and J. Malik. A database of human segmented natural images and its application to evaluating segmentation algorithms and measuring ecological statistics. In *Int. Conf. Computer Vision*, 2001.

D. Martin, C. Fowlkes, and J. Malik. Learning to detect natural image boundaries using local brightness, color, and texture cues. *IEEE Trans. PAMI*, 26:530–549, 2004.

D. Munoz, A. Bagnell, and M. Hebert. Stacked hierarchical labeling. In *European Conf. Computer Vision*, 2010.

N. Payet and S. Todorovic. SLEDGE: Sequential labeling of image edges for boundary detection. *Int. J. Computer Vision*, 104(1):15–37, 2013.

X. Ren, C. Fowlkes, and J. Malik. Learning probabilistic models for contour completion in natural images. *Int. J. Computer Vision*, 77(1-3):47–63, 2008.

S. Ross and A. Bagnell. Efficient reductions for imitation learning. *Journal of Machine Learning Research - Proceedings Track*, 9:661–668, 2010.

S. Ross, G. Gordon, and A. Bagnell. A reduction of imitation learning and structured prediction to no-regret online learning. *Journal of Machine Learning Research - Proceedings Track*, 15:627–635, 2011.

E. Sharon, A. Brandt, and R. Basri. Segmentation and boundary detection using multiscale intensity measurements. In *Conf. Computer Vision Pattern Recognition*, pages 469–476, 2001.

D. Weiss and B. Taskar. Structured prediction cascades. *Journal of Machine Learning Research - Proceedings Track*, 9:916–923, 2010.

L. Williams and K. Thornber. A comparison of measures for detecting natural shapes in cluttered backgrounds. *Int. J. Computer Vision*, 34(2-3):81–96, 1999.

Q. Zhu, G. Song, and J. Shi. Untangling cycles for contour grouping. In *Int. Conf. Computer Vision*, pages 1–8, 2007.

S.-C. Zhu. Embedding Gestalt laws in Markov random fields. *IEEE Trans. PAMI*, 21(11):1170–1187, 1999.